二維心臟超音波左心室分割與其區域運動分析
The Left Ventricular Segmentation and Regional Wall Motion Analysis for Two-Dimensional Echocardiograms

黃樹乾
SHU-CHIEN HUANG
成功大學資訊所
Institute of Information Engineering
Cheng Kung University

孫永年
YUNG-NIEN SUN
成功大學資訊所
Institute of Information Engineering,
Cheng Kung University

林少琳
SHOA-LIN LIN
高雄榮民總醫院
Division of Cardiology,
Veterans General
Hospital-Kaohsiung

摘要

超音波影像是一非侵入性的臨床工具，區域定量分析功能可診斷心肌貧血的嚴重程度。本論文主要以基因演算法爲基礎以擷取心室區域部份，對於去除乳頭肌部份是以先驗知識處理之，實驗結果與測試均顯示此方法的可行性。

關鍵字: 心臟超音波影像; 左心室; 基因演算法, 先驗知識

Abstract

Echocardiography has been widely used as a non-invasive clinical tool to diagnose cardiac functions. The quantitative analysis of regional wall motion provides a useful method for accessing the severity of ischemia and infraction. This paper describes a new boundary extraction method from 2-D echocardiograms, which is based principally on genetic algorithms(GAs). The ambiguity of papillary muscles is processed by a knowledge-based scheme. The method is more stable for the detection of the endocardial border. Experiments on several left ventricular(LV) echocardiograms and clinical validation have shown the effectiveness of our method in these patient studies.

Keywords. Echocardiography; Left Ventricule; Genetic Algorithm; Knowledge-based scheme

1. Introduction

Echocardiography has been used as a major clinical tool due to the relative comfort and safety to the patients. Unfortunately, the main disadvantage of ultrasound echocardiography is relatively poor image quality and high noise levels, and the connective tissues, including papillary muscles and mitral valve inside ventricular chamber, also tend to cause ambiguities in defining the ventricular area. Therefore, the segmentation of endocardial boundaries is important and difficult to achieve. Quantitative analysis of the cardiac function requires the complete determination of the boundaries of the heart wall. The cardiac shape is considered as one of the important parameters which reflect the complex interactions of the electrical and metabolic mechanics. In order to obtain indices of cardiac performance such as ejection fraction and ventricular volume, it is necessary to obtain the contour lines corresponding to the endocardial wall of the heart chamber.

Several researches for detecting ventricular border from 2D Echocardiograms have been reported. Most methods rely on using only the image gray scale information to identify the cardiac border[1-3]. Chu et al.[4] presented a method by using a Laplician of Gaussian operator followed by a radial search method to detect endocardial and epicardial borders. Chou et al.[5] applied a method which extracted the myocardial edge with an ideal echo-intensity image model and relaxation algorithm. Klingler et al.[6] used mathematical morphology operations to detect the left ventricular edge. Friedland et al.[7] developed a system using simulated annealing to compound the spatial and temporal information along with a physical model in the decision rule. The graph searching approach[8] is a robust method for tracing the local edge transitions, but it is also based on local intensity information. Vikram Chalana et al.[9] proposed a multiple active contour model for cardiac boundary detection on echocardiographic sequences, but the user needs to specify manually a rough epicardial boundary on the ED image. In addition to, some researchers make use of fuzzy reasoning[10] and relaxation labeling[11] method for cardiac boundary detection, but these methods do not take into account the presence of papillary muscles in the image.

In this paper, we proposed a new approach to obtain the initial endocardial contour, and genetic algorithm is applied to extract the accurate endocardial borders from 2D echocardiograms. Experimental studies and quantitative analysis

have been performed on several serial LV echocardiograms.

The paper is organized as follows. In the following section describes how to estimate the initial contour for the first image. Genetic algorithm for accurate endocardial border detection will be presented in Section 3. Section 4 describes the experimental results and addresses the quantitative analysis for regional wall motion. Finally, the discussion and conclusion are given in Section 5 and Section 6, respectively.

2. Initial Contour Estimation

The initial contour estimation procedures consist of six modules, as illustrated in Fig.1. First, the approximate ED image is selected as the first image shown in Fig.2(a). We define manually the rectangular region of interest(ROI) for the processing on this image, so that the irrelevant processing time can be eliminated.

A simple 3x3 median filter was applied in our system to reduce the speckle noise, and the result is shown in Fig.2(b). After the process, the Sobel operations and threshold are utilized to produce a binary image(see Fig.2(c)).

Morphological techniques are then applied to estimate the initial endocardial boundary on the first image. The morphological filtering operations can remove the small isolated regions inside the image shown in Fig.2(c). The process consists of opening and closing with a 5x5 structuring element. The result after such opening and closing operations is shown in Fig.2(d).

The phenomenon of dropout in ultrasound images makes the segmentation of LV more difficult. However, most methods do not take the dropout problem into account. In our method, to reduce the impact of these dropout areas of the final segmentation of Fig.2(a), a circular growing operation instead of a pixel aggregation was used to group pixels into LV cavity region. The seed used for circular growing is the center of ROI. The procedure sets the cavity to be black region, and other part to be white region(see Fig.2(e)). However, there is still small white region inside the cavity, so the circular growing operation must be performed again but the seed is chosen randomly from these white pixels outside the cavity. Then the image subtracts the resulting white area is a complete black region without any white region inside it. The resulting image is shown in Fig.2(f).

After the above procedures, we can easily use radial search technique to detect the LV boundary candidate points from Fig.2(f). On every searching line, the nearest border point from the cavity center is selected as a candidate point. After all candidate points(see Fig.2(g)) are determined, the Catnull-Rom spline[12] is used in interpolating these endocardial candidate points. The close endocardial contour is shown in Fig.2(h).

While outlining the endocardial borders, the papillary muscles were considered as a part of the left-ventricular cavity as recommended by the American Society of Echocardiography[13]. The LV endocardial contour like a circle or ellipse. Based on this assumption, we propose to use the distance-angle plot to include the papillary muscles as a part of the LV cavity. It is completed by three steps:

step 1: Calculate distance between center and contour points. and draw the distance-angle plot shown in Fig.3.

step 2: Find the point (P1), whose distance value is maximum between 170° and 190° . Find the point (P2), whose distance value is maximum between 230° and 270° , and find the point (P3), whose distance value is maximum between 50° and 90° .

step 3: Connect P1,P2 and P1,P3 on the distance-angle plot, and maps the distance-angle plot to form an estimated endocardial contour(see Fig.4) that will be used as an initial contour in the subsequent contour refinement process.

3. The Proposed Method

In this section, we propose to use the genetic algorithms[14-16] to further refine the endocardial border shown in Fig.(4). The GA proposed by John Holland[15] and it is an adaptive procedure that searches for good solutions by using a collection of search points known as a population in order to maximize a user-defined function called the fitness function.

GA is a powerful tool for solving problems which involves a search processing through a complex solution space. Because GAs use population-wide search instead of a point-search, and the transition rules of GAs are stochastic instead of deterministic, the probability of reaching a false peak in GAs is much less than one in other conventional searching schemes.

3.1 Encoding scheme of chromosome

Fig.5 gives an example of encoding mechanism. The rough boundary obtained from initial contour estimation is first uniformly sampling into M` points. A sampled point is associated with a line segment which is perpendicular to the contour and passing through these sampled point. In our algorithm, the line segment will be eliminated if the gray scale

variance of all points in this line segment is less than a given threshold value. These eliminated line segments usually locate near the papillary muscle or the dropout region. After the elimination process, there are M(M ≤ M') line segments survive. On each line segment, K grid points are given from which the cardial border point is to be detected. For line segment L_i, if the detected border point is the j^{th} point, we then denote $G_i=j$ to indicate that the j^{th} point is the resulting border point on the i^{th} line segment.

3.2 Fitness function

The fitness of each chromosome is computed for each generation in order to eliminate non-effic nt chromosomes in the next generation. The chromosome with higher fitness value represents a better solution. For a chromosome S, if the set of the chosen ventricular points is $\{V_1, V_2, V_3, \ldots V_{M-1}, V_M\}$ where $V_i \in L_i (i=1,2 \ldots M)$. The fitness value of chromosome S can be defined as follows:

$$F(S) = \sum_{i=1}^{M} e(V_i) = \sum_{i=1}^{M} (\alpha E_1^i + \beta E_2^i + \gamma E_3^i) \quad (1)$$

where,

$$E_1^i = \frac{1}{2}(1 - \cos(\theta)),$$

$$E_2^i = \frac{|\nabla I(V_i)|}{\underset{V \in L_i}{Max}(|\nabla I(V)|)},$$

$$E_3^i = \frac{P(V_i)}{\underset{V \in L_i}{Max}(|P(V)|)}$$

Here, $e(V_i)$ is the fitness value of the point V_i. The first term E_1 is the curvature, and θ is the bending angle at V_i. Thus $-1 \le \cos\theta \le 1$, and $E_1=1$ for a straight line(180^0), and 0 for the sharpest angle(0^0).

In the second term E_2 is gradient. $\nabla I(V_i)$ is the image intensity gradient of point V_i, and this term is normalized by dividing by the largest gradient value of the point, on the given line segment, thus E_2 is a number from 0 to 1.

In the third term E_3 is contrast. The contrast magnitude of the point V_i, denoted by $P(V_i)$, is defined by

$$P(V_i) = \sum_{j=w4}^{j=w6} I(V_j) - \sum_{j=w1}^{j=w3} I(V_j) \quad (2)$$

Here $I(V_i)$ is the intensity of the point V_i. $P(V_i)$ is the contrast computed in a window on a search perpendicular to the contour. In echocardiographic images, the darker areas correspond to cavity region and the brighter areas normally correspond to the heart or muscle tissues. The point with larger contrast magnitude indicates that it is a better LV boundary point. Therefore, this term is designed to be related with the priori knowledge.

3.3 Selection

In the selection process, a roulette wheel is utilized where each chromosome in the population has a slot with size in proportion to its fitness. The probability that chromosome S_i (i=1,2,...pop_size) is selected as a member of the next generation is

$$P_i = \frac{F(S_i)}{\sum_{j=1}^{pop\_size} F(S_j)}, \quad (3)$$

where pop_size is the population size. The pop_size selected chromosomes are then entered into a mating pool, for further genetic operations.

3.4 Crossover

The information exchange of the crossover operation gives much of the power in genetic algorithms. In the crossover operation, two cut points are chosen at random and chromosomal material between the two cut points is swapped between the two mating chromosomes. For example, X and Y are two chromosomes to be mated:

$X=x_1x_2x_3 \ldots x_kx_{k+1} \ldots x_t \ldots x_m$

$Y=y_1y_2y_3 \ldots y_ky_{k+1} \ldots y_t \ldots y_m.$

If two positions k and t are selected to do crossover, their offspring after mating will be:

$X'=x_1x_2x_3 \ldots y_ky_{k+1} \ldots y_t \ldots x_m$

$Y'=y_1y_2y_3 \ldots x_kx_{k+1} \ldots x_t \ldots y_m.$

3.5 Mutation

In natural terminology, chromosomes are composed of genes, which may take on some number of values called alleles. Mutation involves modification of the values of genes in a chromosome; In the mutation operation, each allele in each chromosome is changed randomly with an equal chance.

The mutation is to change the position of candidate points. For each line segment $L_i (1 \le i \le M)$, a point $V_i(new)$ is chosen as a new candidate point according to the following rule:

$$V_i(new) = \arg\max_{V \in L_i} e(V). \quad (4)$$

Therefore, the index number of point $V_i(new)$ is given to G_i. It can be shown that after each mutation operation the new fitness value F(S(new)) is greater than the original fitness value, i.e.,

$F(S(new))=e(V_1)+e(V_2)+\ldots+e(V_{i-1}) + e(V_{i(new)}) +\ldots+e(V_m) \ge e(V_1) + e(V_2) +\ldots+ e(V_{i-1}) + e(V_i)+\ldots+ e(V_m)=F(S).$ (5)

In this operation, the selected point is the one with maximum energy that is the same as the operation in the conventional greedy method[18].

However, the GA mechanism makes the energy optimization in an iterative manner with stochastic global adjustment, that includes selection, crossover and mutation.

3.6 The proposed genetic algorithm

step.1 Construct an initial chromosome population A.
f*=F(M*), where M* represents the best chromosome in A.
g=g*=1, where g represents the current generation number and g* denotes the generation number when the best chromosome is first found.

Step.2 Calculate the value of fitness function for each chromosome in the current population A.

Step.3 Perform reproduction, crossover and mutation, and the new population O is generated.
Update the generation number g=g+1.

Step.4 Assume A_{best} and B_{worst} are the best chromosome in the population A and the worst chromosome in the population O, respectively.
$A=(O-\{B_{worst}\})\cup\{A_{best}\}$.

Step.5 Assume M' is the best chromosome in the new population A.
If f(M') is greater than f*
{ M*=M'; f*=F(M'); g*=g; }
else if g - g* is greater than a threshold t*=10, Goto step 6;
else Goto step 2.

Step.6 Output the best chromosome M* which represents the actual endocardial boundary points, and the Catnull-Rom spline is used in interpolating these endocardial boundary points.

4. Experimental Results and Quantitative Analysis

Ultrasonic images were acquired from a HP-1500 ultrasonic system at Veterans General Hospital-Kaohsiung. The processing was performed on a Sun Sparc 20. The system has been tested for twelve cases of clinical studies. We utilize the detected contour on the present frame to detect the border on the next frame throughout the whole cardial cycle. By tracing the wall motion at end-diastole and end-systole, the regional wall motion can therefore be analyzed and displayed. Figure 6 shows the segmentation results from the sequence of some patient's echocardiograms and the system takes 35 seconds to detect one cycle of endocardial borders.

The segmental nature of coronary artery disease leads to segmental defects in left ventricular function. With frank infarction the ventricular defect may cause a significant change in global ventricular function with a decrease in ejection fraction and a qualitatively obvious angiography abnormality. Therefore, it is needed to develop analysis tools for doctors to recognize LV regional wall motion[17]. After the method detects one cycle endocardial borders, the quantitative analysis charts can be displayed immediately. We develop three kinds of quantitative analysis charts.

1). Area curve
The LV endocardial area is calculated for each frame. Comparison of left ventricular area measurements obtained by our method versus those obtained by a physician is shown in Fig.7.

2). Shortening fraction(S.F.) analysis
Fig.8 shows the graphic expressions of end-diastole(E.D.) and end-systole(E.S.), and we can define a radial line each 3 degrees clockwise. For a radial line L, its shortening fraction is (a-b)/a. The resulting shortening fraction calculated from the segmentation results is plotted in Fig.9.

3).The regional area change
The left ventricle was divided into eight 45° wedge-shaped segments(Fig.10). For some segment R, its area change is A/(A+B). The resulting area change calculated from the segmentation results is plotted in Fig.11.

5. Discussion

In this paper we have attempted to address a boundary detection problem in a very difficult domain, echocardiography. It is this domain which has made the design of a robust and efficient algorithm using classic image processing methods inadequate.

The novelty of this algorithm is the implementation of the GA optimization method in detecting ultrasound image cavity boundaries from a sequence of input images. The major concern in this method was the selection of the appropriate control parameters for the GA. It has been pointed out in [16] that the population size ranged from 10 to 160, the crossover rate ranged from 0.25 to 1.00, and the mutation rate ranged from 0.0 to 1.0. A small population may cause premature convergence to suboptimal solutions. On the other hand, a large population requires more evaluations per generation. In the current experiments, the population size is fixed to 100.

The crossover rate controls the frequency of crossover operation. The higher the crossover rate, the more quickly new structures are generated into the population. If the crossover rate is too low, the

search may stagnate due to the lower exploration. The crossover rate is fixed to 0.4 in our experiments.

In this application the mutation rate(P_m) is also used as an important parameter. We tried value of P_m ranging from 0.1 to 1.0 with increment of 0.05. The mutation rate is empirically fixed to 0.15, since it is an appropriate value to prevent premature convergence to suboptimal solutions and to provide the best results with high speed of convergence.

6. Conclusion

A new method for endocardial border detection has been presented, whose operations utilize the knowledge imbedded in the models. This method is superior to other methods in three ways. First, the GA approach provides a robust and good method for the detection of endocardial boundaries. Secondly, the algorithm is capable of handling the inherent problems of image-dropout in echocardiograms. Thirdly, The resulting endocardial boundaries include the papillary muscles as a part of the LV cavity, whereas most other studies have concentrated on detecting the blood-tissue interface excluding the papillary muscles. The three advantages make our system more desirable for the detection of the endocardial border.

Additionally, we proposed three kinds of quantitative analysis charts for regional wall motion. Therefore, the proposed image analysis system provides an important tool for the clinical evaluation and diagnosis of cardiac diseases. Such an image processing tool can help the cardiologist to evaluate the severity of cardial disease quantitatively and promptly.

References

1. H.E. Melton, S.M. Collins, and D.J. Skorton, "Automatic real-time endocardial edge detection in two-dimensional echocardiography," Ultrason. Imag., vol.5, pp.300-307, 1983.
2. P.R. Detmer, G.Bashein, and R.W. Martin, "Matched filter identification of left-ventricular endocardial borders in transeophageal echocardiograms," IEEE Trans. Med. Imag., vol.9, pp.396-404, 1990.
3. S. Tamura and K. Yata, "Plan-based boundary extraction and 3-D reconstruction for orthogonal 2-D Echocardiography," Pattern Recognition, pp.155-162, 1987.
4. C.H. Chu, E.J. Delp and A.J. Buda, " Detecting left ventricular endocardial and epicardial boundaries by digital two-dimensional Echocardiography", IEEE Trans. Med. Imag., MI-7, pp.81-90, 1988.
5. W.S. Chou, C.M. Wu, Y.C. Chen , K.S. Hsien, "Detecting Myocardial boundaries of Left Ventricular from a single frame 2DE image", Pattern Recognition, Vol. 23, No. 7, pp. 799-806, 1990.
6. J.W. Klingler, C.L. Vaughan, T.D. Fraker and S.Zhuang, "Segmentation of echocardiographic images using mathematical morphology", IEEE Trans. Biomedical Engineering, BME-35 pp. 925-934, 1988.
7. N.Friedland and D.Adam, "Automatic ventricular cavity boundary detection from sequential ultrasound images using simulated annealing," IEEE Trans. medical imaging, vol.8, no.4, pp.344-353, 1989.
8. Daniel R. Thedens, David J. Skorton, and Steven R. Fleagle, "Methods of graph searching for border detection in image sequences with applications to cadiac magnetic resonance imaging," IEEE Trans. medical imaging, vol.14, no.1, pp.42-55, 1995.
9. Vikram Chalana, David T.Linker, David R.Haynor, and Yongmin Kim, "A multiple active contour model for cardiac boundary detection on echocardiography sequences," IEEE Trans. medical imaging, vol.15, no.3, pp.290-298, 1996.
10. J.Feng, W.Ling, and C.Chen, "Epicardial boundary detection using fuzzy reasoning," IEEE Trans. medical imaging, vol.10, pp.187-199, 1991.
11. T.Faber, E.Stokley, R.Peshock, and J.Corbett, "A model-based four-dimensional left ventricular surface detector," IEEE Trans. medical imaging , vol.10, pp.321-329, 1991.
12. J. Foley, A.V. Dam, S.Feiner and J.Hughes, Computer Graphics Principles and Practice, 2nd Edn. Addison-Wesley, Reading, Massachusetts, 1990.
13. N. Schiller, P. Shah, M. Crawford, A.DeMaria, R.Devereux, H.Feigenbaum, H. Gutgesell, N. Reichek, D.Sahn, I.Schnittger, N.Silvermam, and A. Tajik, "Recommendations forquantitation of the left ventricle by two-dimensional echocardiography: American society of echocardiography committee in standards subcommittee," J.Amer. Soc. Echocardiogr., vol.2, pp.358-367, 1989.
14. D.E. Goldberg. Genetic Algorithms in Search, Optimization and Machine Learning, Addison-Wesley. Reading, Mass., 1989.
15. J.H. Holland, Adaptation in Natural and Artificial Systems, Univ. of Michigan Press. Ann Arbor, Mich., 1975.
16. J.J. Grefenstette, "Optimization of Control Parameters for Genetic Algorithms," IEEE Trans. Systems, Man, and Cybernetics, Vol. SMC-16, no.1, pp.122-128, 1986.
17. R.M. Lang, P. Vignon, L. Weinert, J. Bednarz, C. Korcarz, J. Sandelski, and R. Koch, "Endocardiographic Quantification of Regional Left Ventricular Wall Motion With Color Kinesis," Circulation , pp.1877-1885, 1996.
18. D.J. williams and M. Shah, "A fast algorithm for active contours," In Proc. of international Conf. on Computer Vision, pp.592-596, 1990.

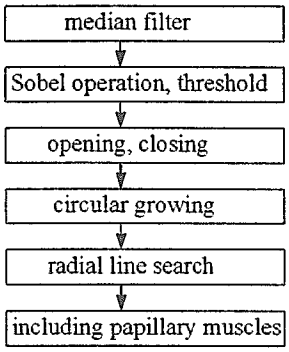

Fig.1 The flowchart for initial estimation

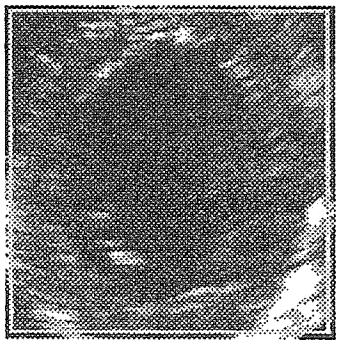

Fig.2(a)

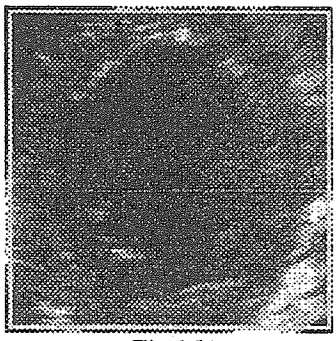

Fig.2(b)

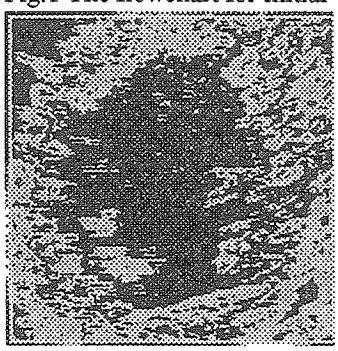

Fig.2(c)

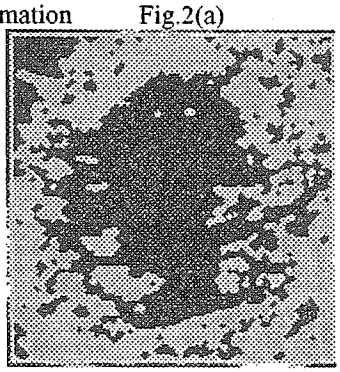

Fig.2(d)

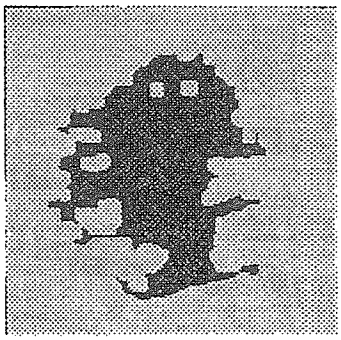

Fig.2(e)

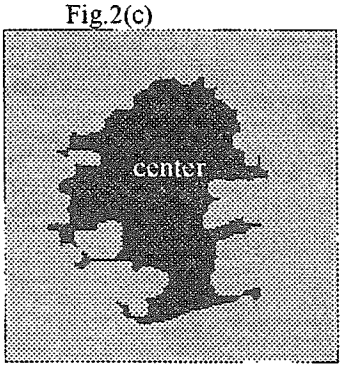

Fig.2(f)

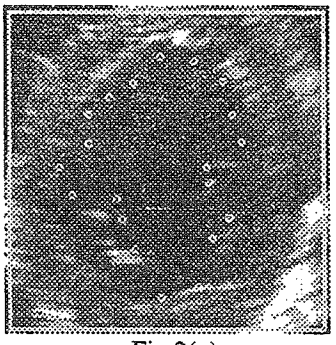

Fig.2(g)

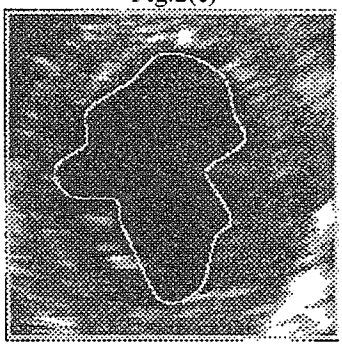

Fig.2(h)

Fig.2 (a) An original echocardiogram. (b) Processed image after median filter. (c) Processed image after Sobel and threshold operations. (d) Processed image after opening and closing. (e) Processed image after the first circular growing operation. (f) Processed image after the second circular growing operation. (g) The endocardial candidate points superimposed on Fig.2(a). (h) The initial endocardial border excluding papillary muscles.

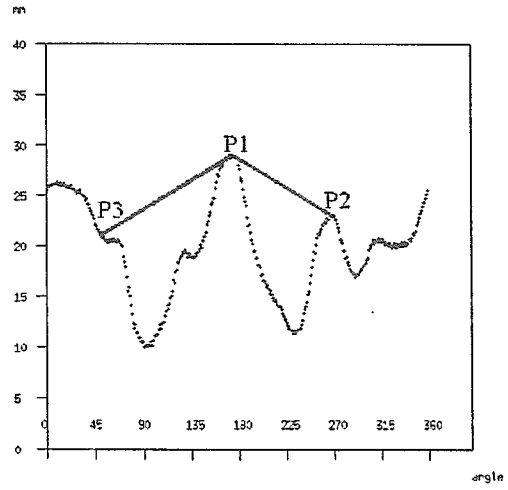

Fig.3 The distance-angle plot

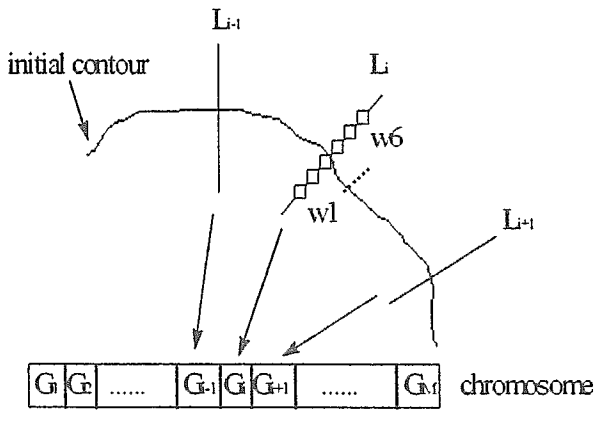

Fig.5 An example of chromosme structure.

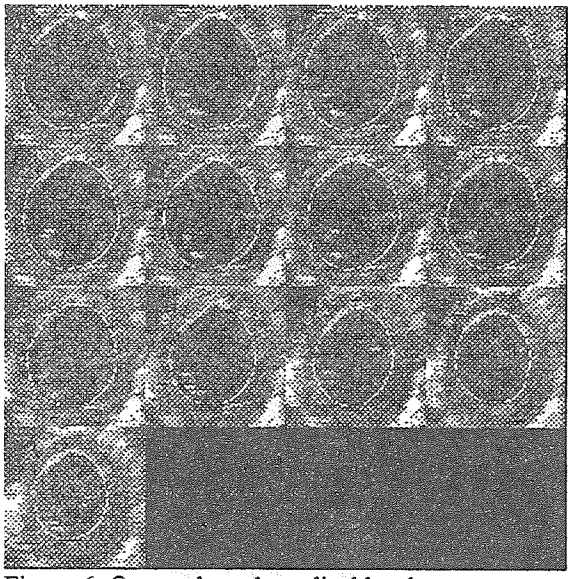

Figure 6. One cycle endocardical borders

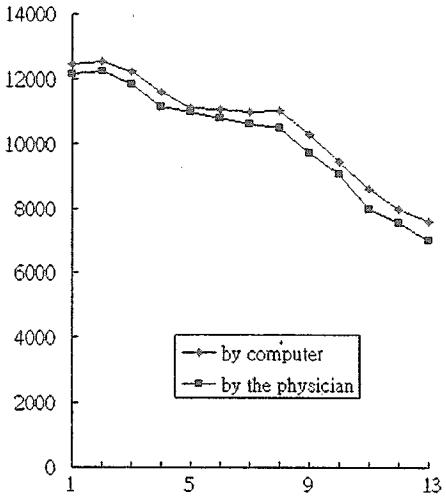

Figure 7. The graph of ventricular area with respect to frame number.

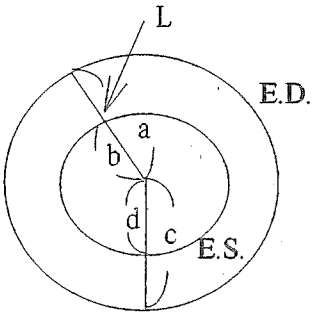

Fig.8 The shortening fraction

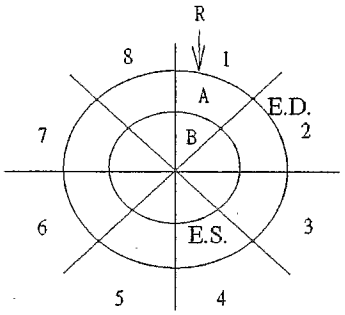

Figure 10. The eight 45° wedge-shaped segments

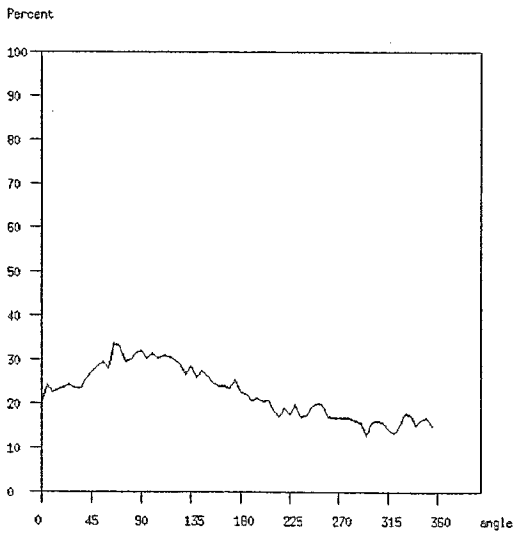

Fig.9 The shortening fraction

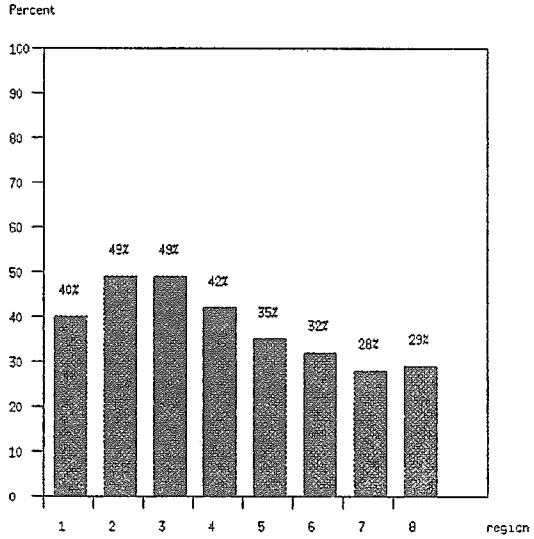

Figure 11. The regional area change